# Distinct populations of neurons respond to emotional valence and arousal in the human subthalamic nucleus

Tomáš Sieger[a,b,1], Tereza Serranová[a,1], Filip Růžička[a], Pavel Vostatek[b], Jiří Wild[b], Daniela Šťastná[c], Cecilia Bonnet[a], Daniel Novák[b], Evžen Růžička[a], Dušan Urgošík[c], and Robert Jech[a,2]

[a]Department of Neurology and Center of Clinical Neuroscience, First Faculty of Medicine and General University Hospital, Charles University in Prague, 128 21, Prague, Czech Republic; [b]Department of Cybernetics, Faculty of Electrical Engineering, Czech Technical University in Prague, 166 27, Prague, Czech Republic; and [c]Department of Stereotactic and Radiation Neurosurgery, Na Homolce Hospital, 150 30, Prague, Czech Republic

Edited by Joseph E. LeDoux, New York University, New York, NY, and approved January 27, 2015 (received for review June 10, 2014)

**Both animal studies and studies using deep brain stimulation in humans have demonstrated the involvement of the subthalamic nucleus (STN) in motivational and emotional processes; however, participation of this nucleus in processing human emotion has not been investigated directly at the single-neuron level. We analyzed the relationship between the neuronal firing from intraoperative microrecordings from the STN during affective picture presentation in patients with Parkinson's disease (PD) and the affective ratings of emotional valence and arousal performed subsequently. We observed that 17% of neurons responded to emotional valence and arousal of visual stimuli according to individual ratings. The activity of some neurons was related to emotional valence, whereas different neurons responded to arousal. In addition, 14% of neurons responded to visual stimuli. Our results suggest the existence of neurons involved in processing or transmission of visual and emotional information in the human STN, and provide evidence of separate processing of the affective dimensions of valence and arousal at the level of single neurons as well.**

emotion | basal ganglia | subthalamic nucleus | single neuron | arousal

At one time, the subthalamic nucleus (STN), which is an important target for deep brain stimulation (DBS) in the treatment of motor symptoms in Parkinson's disease (PD), was considered an important regulator of motor function (1, 2); however, the occurrence of postoperative neuropsychiatric complications has expanded interest in the nonmotor function of the STN (3, 4). Animal and human studies have already demonstrated the additional functional role of the STN in emotional and motivational processes (5–12). In addition, recent functional MRI studies found STN activation in response to emotional stimuli in healthy subjects (13, 14). Therefore, we hypothesized that emotional activity-related neurons should exist in the STN. Participation of the STN in processing emotion has not yet been investigated directly at the single-neuron level in humans. Nonetheless, single-neuron activity related to a priori defined emotional categories (e.g., positive vs. negative) has been detected in a few human brain regions, including the hippocampus, amygdala, and prefrontal and subcallosal cortex (15–18).

It has been proposed that emotional behavior is organized along two psychophysiological dimensions: emotional valence, varying from unpleasant to pleasant, and arousal, varying from low to high (19). The individual assessment of these dimensions is closely correlated with somatic and autonomic measures of emotions (20, 21). Contrary to a priori categories, they can better reflect emotional characteristics of the stimulus in an individual context, and they take into account interindividual differences based on specific behavioral determinants, such as affective disposition and personality traits (22).

In this study, we aimed to detect single-neuron firing pattern changes in the STN that are related to emotional arousal and valence from the individual ratings of emotionally charged and neutral pictures presented to PD patients undergoing DBS electrode implantation. It has been shown that different features of tasks are linked to neuronal activity in different frequency bands. Whereas beta band oscillations (13–30 Hz) restricted to the dorsolateral (sensorimotor) part of the STN are linked mainly to motor functions and their alteration in PD (23–25), the gamma band oscillations (30–100 Hz) perhaps have a more general meaning. Along with motor functions, they are modulated by picture perception and early emotional arousal (26, 27). Because we were interested in the affective content of visual processing, we focused on the alpha oscillations (8–12 Hz), because they repeatedly showed emotion-related behavior in local field potential (LFP) recordings (7, 28, 29). We used the power spectra bands, which are well known in descriptions of continuous LFP and EEG signals that we adopted for analysis of the discrete single-neuron signal from the STN during the task with affective picture presentation.

In this study, we compared the individual alpha firing activity of single neurons with specific affective experiences expressed in subjective ratings of the emotional valence and arousal of each presented picture, and then mapped these neurons into the STN model (30). A neuron was classified as affective if its history-adjusted (and category-adjusted) activity in the alpha band correlated with these ratings.

Studies of spatiotemporal dynamics of emotions (affective picture or facial emotion processing) have observed early and late changes that have been attributed to different stages of emotional processing

## Significance

**The involvement of the subthalamic nucleus (STN) in affective processing has been suggested with the appearance of neuropsychiatric side effects of deep brain stimulation in Parkinson's disease (PD), but direct evidence has been lacking. In our study, we recorded single-neuron activity from the STN during affective picture presentation to PD patients intraoperatively. We discovered two spatially distinct populations of "affective" neurons responding to the emotional dimensions of the stimuli: valence (pleasantness-unpleasantness) and arousal (intensity). As previously believed, neural circuits underlying these two affective dimensions are functionally segregated. Here we observed separated emotional processing even at the single neuron level. These results extend our knowledge regarding the emotional role of the STN and the neural basis of emotions.**

Author contributions: T. Sieger, T. Serranová, and R.J. designed research; T. Serranová, F.R., E.R., D.U., and R.J. performed research; T. Sieger and P.V. contributed new reagents/analytic tools; T. Sieger, T. Serranová, F.R., P.V., J.W., D.Š., C.B., and D.N. analyzed data; and T. Sieger, T. Serranová, and R.J. wrote the paper.

The authors declare no conflict of interest.

This article is a PNAS Direct Submission.

Freely available online through the PNAS open access option.

[1]T. Sieger and T. Serranová contributed equally to this work.

[2]To whom correspondence should be addressed. Email: jech@cesnet.cz.

This article contains supporting information online at www.pnas.org/lookup/suppl/doi:10.1073/pnas.1410709112/-/DCSupplemental.

**Table 1. Patients' and normative ratings of emotional stimuli used**

| | Patients' rating | | Normative rating | |
|---|---|---|---|---|
| Category | Valence, mean (SD) | Intensity, mean (SD) | Valence, mean (SD) | Intensity, mean (SD) |
| Negative | 3.1 (1.6) | 5.1 (2.6) | 3.4 (0.7) | 5.2 (1.1) |
| Neutral | 5.2 (1.0) | 2.6 (1.7) | 5.0 (0.2) | 2.8 (0.3) |
| Positive | 6.0 (1.3) | 4.0 (2.1) | 6.6 (0.8) | 5.2 (1.1) |

Patients' ratings represent subjective ratings assessed at 1 mo after bilateral insertion of the permanent electrode into the STN after overnight withdrawal of levodopa in the DBS-off condition. Normative ratings are those available from the IAPS (80).

(31–33). Therefore, for our analysis, we arbitrarily split the picture observation period of 2 s into two time windows. Within the early window (0–500 ms), which may contain early emotional images confounded more by perceptual and attentional processes (31, 33–37), we searched for activity related to the affective picture presentation in contrast to the black screen periods preceding each picture. For emotional activity, we searched in the late window, starting at 500 ms after the visual stimulus onset, because this can be better related to emotional processing after the conceptual knowledge of the presented emotion (represented here in individual ratings of the emotional valence and arousal) is built (32).

## Results

We recorded single-neuron activity in the STN from 13 PD patients intraoperatively performing an affective task consisting of a presentation with pleasant, unpleasant, and neutral pictures displayed for 2,000 ms, preceded by a black screen with a white fixating cross presented for 3,500–5,500 ms. We acquired 97 microelectrode recordings obtained from 47 sites in the STN, in which a total of 125 neurons were detected. The activity of 35 neurons was related to eye movements, and these neurons were excluded from further analysis. The remaining 90 neurons (71 in the left hemisphere) were searched for early perceptual and emotional characteristics. Normative and postoperatively recorded individual valence and arousal ratings for each picture category are presented in Table 1.

The alpha band activity of 15 of 90 neurons (17%) during the late period of picture presentation epochs (500–2,000 ms after stimulus onset) was related to the emotional content of the presented pictures expressed in individual valence or arousal ratings ($P < 0.05$, uncorrected). The activity of six neurons (7%) correlated with the valence ratings (four neurons negatively, two neurons positively; Fig. 1). The activity of other nine neurons (10%) correlated with the arousal ratings (seven neurons positively, two neurons negatively; Fig. 2). Ten of these neurons were located in the left STN, and the other five were located in the right STN, with no interhemispheric differences ($\chi^2 = 0.854$; df = 1; $P = 0.36$). These 15 emotion-related neurons were more than was expected by chance (test in binomial distribution with a false-positive rate of 0.1; $P < 0.05$). Fig. S1 shows how alpha band activity was derived in one selected neuron associated with the arousal rating.

In addition, 13 neurons (14%) demonstrated significantly altered alpha band activity between the black screen (2,000-ms duration) and the early picture presentation (window 0–500 ms after stimulus onset) ($P < 0.05$). Only one neuron exhibited altered alpha band activity in both the early and late time windows.

The locations of the neurons sensitive to emotional content are depicted in Fig. 3. The valence-related neurons in the STN were located more posteriorly compared with the arousal-related neurons ($P < 0.05$, permutation test). The anterior–posterior difference in the mean position of the neuronal populations was 1.9 mm.

In post hoc analyses, we searched for emotion-related neuronal activity in other frequency bands. Four neurons were related to arousal and no neurons were related to valence in the beta band, but their numbers were insignificant ($P = 0.98$, binomial test). In the gamma band, seven neurons were related to arousal and no neurons were related to valence, again not significant ($P = 0.81$, binomial test). No overlaps of beta and gamma emotion-related neurons with alpha emotion-related neurons were observed.

To support the specificity of emotion-related neurons located in the STN, we analyzed the activity of 32 other eye movement-unrelated neurons in other basal ganglia, including 18 neurons from the substantia nigra pars reticulata (recorded from patients 1, 3, 5, 6, 7, 11, 12, and 13; Table 2) and 14 neurons from the globus pallidus (Table S1). None of these neurons was related to individual valence or arousal ratings of the presented pictures.

## Discussion

Using perioperative microrecordings from the STN of patients with PD, we analyzed changes in the firing patterns of single neurons in relationship to visually presented emotional material, and found a relatively large proportion of neurons with activity related to emotional and early perceptual processing. In addition, we showed how easy it is to transform the single-neuron action potentials to a pseudocontinuous signal to perform spectral analysis typical for conventional electroencephalography. Using this approach, we documented the impact of a visual emotional task on single-neuron activity in the alpha band similar to those previously shown with LFPs (7, 28).

**Affective Neurons in the STN.** In this study, 17% of the STN neurons analyzed for activity in the alpha band responded to emotional stimuli. Different neurons responded to changes in emotional valence or in arousal ratings. Figs. S2 and S3 support this finding visually by showing that the valence-related neurons were mostly uncorrelated with arousal and vice versa. As for the character of changes in neuronal activity, both increases and decreases were observed in both populations of neurons, suggesting a further level of specialization within each emotional dimension. There is a large body of evidence suggesting that behavioral responses to emotional valence and arousal are mediated by different brain circuits. The independence of valence

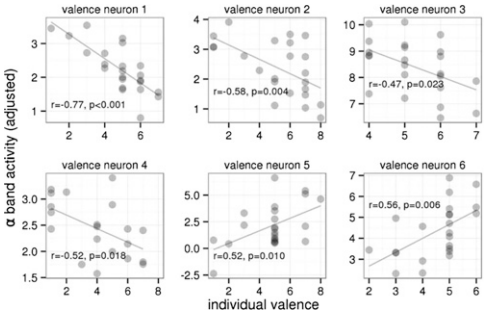


**Fig. 1.** Relationship of the single-neuron alpha band activity during emotional picture presentation (in the interval of 500–2,000 ms after picture onset) to individual valence ratings of the presented pictures in six neurons of the STN in patients with PD, in which the relationship was significant (as identified by linear models; *Experimental Procedures*). In none of these neurons was the activity related to individual arousal ratings (Fig. S2). The horizontal axis shows the individual ratings of the pictures' valence, varying from 1 (unpleasant) to 9 (pleasant). The vertical axis shows the alpha band neuronal activity adjusted for the past activity (Experimental Procedures). For visualization purposes, correlation coefficients and their significance are included.

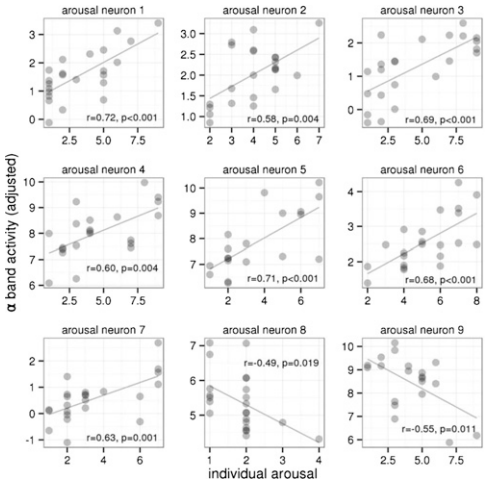


**Fig. 2.** Relationship of the single-neuron alpha band activity during emotional picture presentation (in the interval of 500–2,000 ms after picture onset) to individual arousal ratings of the presented pictures in nine neurons of the STN in patients with PD, in which the dependency was significant (as identified by linear models; *Experimental Procedures*). In none of these neurons was the activity related to individual valence ratings (Fig. S3). The horizontal axis shows the individual ratings of the pictures' arousal, varying from 1 (low) to 9 (high). The vertical axis shows the alpha band neuronal activity adjusted for the past activity and picture categories (*Experimental Procedures*). For visualization purposes, correlation coefficients and their significances are included.

and arousal has already been demonstrated for a variety of physiological reactions (21, 38, 39) and in affect-related cognitive processing (40). Functional imaging and animal studies also have demonstrated their functional segregation, with several brain regions associated with affective valence (eg, orbitofrontal cortex, mesolimbic dopamine system) and others associated with affective arousal (eg, amygdala, mesencephalic reticular activating system) (41–45); however, there is also evidence indicating that the two emotional dimensions are not fully independent (46), and that some subcortical regions may code the overall emotional value of a stimulus (47).

The neuronal activity in the STN that we observed in the late window (500–2,000 ms) may reflect the formation of conceptual knowledge related to emotional valence and arousal, because this is in line with the late neuronal response (625–1,500 ms) related to different valences of stimuli already described in the amygdala (18). We may speculate that the information represented in ratings of emotional valence and arousal in the late time window depends on processes involving the orbitofrontal and ventromedial prefrontal cortex, which provide significant input to the STN and play a major role in stimulus subjective valuation, representation of hedonic pleasure and value-based decision making (48–51). In addition, the previous passage of emotional information from the ventral basal ganglia involving input from the amygdala to the dorsal basal ganglia, including the dorsal portion of the STN, also may be a reason for late emotional activity (52, 53).

As expected, we did not find a statistically sufficient number of neurons responding to the emotional valence and arousal in the beta and gamma frequency bands. This corresponds with the negative results of previous LFP studies (7, 29) and further corroborates the functional specialization of different frequencies within the STN. In addition, we found no neurons responding to emotional content in the globus pallidus or substantia nigra pars reticulata, suggesting that the finding of affective neurons is specific to the STN, explained by its central position in the corticobasal ganglia circuit (54–57) and its connections to both the cortical and the subcortical components of the reward and limbic circuits (53, 58–63).

Despite the previously suggested emotional network asymmetry of both hemispheres (64, 65), the roles of the right and left STN in affective processes are unclear (66, 67). We did not detect any interhemispheric difference in proportion of the emotion-related neurons between the left and right STN; however, this result could have been affected by the limited number of recordings obtained from the right STN.

**Localization of Affective Neurons Within the STN.** A once widely held assumption is that the STN is divided into three functional zones within the STN: limbic, associative, and sensorimotor regions, residing in the anteromedial, middle, and dorsolateral portions, respectively, of the STN (58, 68, 69). This concept has been challenged by several recent electrophysiologic, neuroanatomic, and neuroimaging studies showing incomplete separation of the subthalamic territories (56, 63, 70, 71). Therefore, it is not surprising that the affective neurons were found in the sensorimotor regions, suggesting that motor and nonmotor regions overlap in the STN. In addition, the affective neurons were distributed differently, with the valence-related neurons located more posteriorly and the arousal-related neurons located more anteriorly, supporting the idea that emotional processing is spatially segregated within the STN (Fig. 3). In this study, however, because we were limited by the parkinsonism-improving implantation procedure, the microrecording was restricted predominantly to the lateral portion of the STN; therefore, we cannot rule out the presence or different spatial distribution of affective neurons in the medial part of the STN (Fig. 3).

**Perceptual Neurons in the STN.** Fourteen percent of the subthalamic neurons responded in the alpha band firing activity during the early time window (0–500 ms), suggesting their connection with perceptual processing. Neuronal short-latency activity changes related to visual perception have already been found in animal STNs (72–74), and have been confirmed in humans by distortion of visual evoked potentials due to STN DBS (75). The difference in neural activity between the fixation and picture viewing periods is not necessarily evidence of visual processing, however; it also may reflect other processes, such as an engagement of selective attention, a shift from gaze fixation to scanning eye movements, or other cognitive functions intervening between vision and action, including memory involvement, target selection,

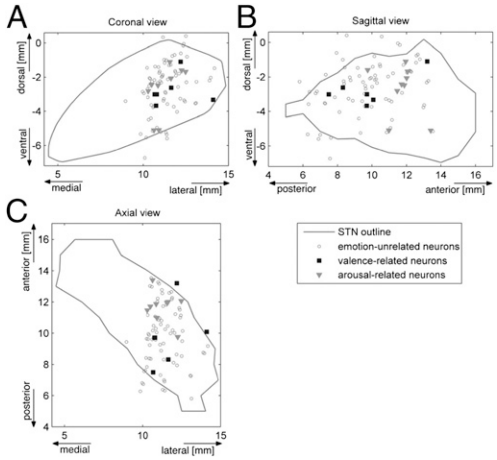


**Fig. 3.** Locations of STN neurons related to emotional content of the presented pictures in coronal (*A*), sagittal (*B*), and axial (*C*) views of the STN model (30) (Fig. S4). The valence-related neurons were located more posteriorly compared with the arousal-related neurons.

**Table 2. Descriptive data of PD patients with STN neuronal activity explored**

| Patient | Age, y | DD, y | Preoperative levodopa, mg | UPDRS-III score | Neurons, n | Emotion-related neurons, n |
|---|---|---|---|---|---|---|
| 1 | 64 | 14 | 1,375 | 31 | 8 | 1 |
| 2 | 61 | 14 | 1,200 | 37 | 5 | 0 |
| 3 | 46 | 15 | 1,000 | 40 | 10 | 1 |
| 4 | 63 | 30 | 1,250 | 50 | 2 | 1 |
| 5 | 53 | 12 | 700 | 37 | 7 | 1 |
| 6 | 69 | 9 | 750 | 47 | 2 | 0 |
| 7 | 49 | 12 | 1,550 | 65 | 4 | 1 |
| 8 | 53 | 11 | 1,663 | 45 | 5 | 1 |
| 9 | 64 | 17 | 1,500 | 31 | 11 | 2 |
| 10 | 42 | 9 | 740 | 33 | 16 | 3 |
| 11 | 55 | 19 | 1,980 | 35 | 8 | 2 |
| 12 | 60 | 14 | 1,060 | 18 | 7 | 0 |
| 13 | 43 | 9 | 1,100 | 34 | 5 | 2 |

Age refers to age on the day of surgery; DD, PD duration; preoperative levodopa, dose/day in mg, including levodopa-equivalent dosage of dopamine agonist (patient 4 was also treated with mianserin, and patients 6, 7, 12, and 13 were also treated with citalopram); UPDRS-III, motor score of the Unified Parkinson´s Disease Rating Scale in the off-medication condition; neurons, number of subthalamic neurons unrelated to eye movements; emotion-related neurons, number of neurons responding to emotional stimuli.

saccade choice, and content valuation (76). On the other hand, the neuronal activity in the early time window also could be affected by early emotional and motivational activity.

The STN is anatomically connected to subcortical centers that contain visually responsive neurons (i.e., superior colliculus, pulvinar, amygdala, substantia innominate, and nucleus accumbens) involved in the visual encoding of emotional stimuli (73, 77). Given that the visual, attentional, and emotional systems are intensively interconnected, some proportion of the affective neurons also might be expect to respond in the early time window; however, here only one of the neurons was activated during both the early and late time windows. Therefore, we can speculate that distinct populations of neurons are involved at different stages of processing of the visual emotional material within the dorsolateral part of the STN.

**Limitations.** Several factors could affect our results and reduce the inferences that can be drawn with regards to the physiology of emotional processing and the role of the STN in the limbic circuits. One such factor is that the study was conducted with PD patients, who are known to have a widespread central nervous system pathology (78) and to experience problems in emotional processing (79), and thus the number of neurons responding to emotional stimuli in the STN might be different from that in healthy subjects. Their number is rather low, but nonetheless is comparable to that reported in previous relevant single-neuron studies on emotion in humans (15, 18). Another factor that might have contributed to the relatively low number of neurons is that the study was limited to the routine trajectory of intraoperative microrecording exploration targeting the lateral sensorimotor part of the STN, which has shown less reactivity to emotional stimuli than the ventromedial part (67). Moreover, emotional pictures were selected according to normative ratings that were acquired in a healthy, younger population with a different cultural background and were partially heterogeneous with respect to visual and emotional content. Finally, some our PD patients rated the stimuli less variable along the dimensions of emotional valence and arousal, making the mathematical model less sensitive (80).

## Conclusion

Early-perceptual and late-emotional single-neuron activity in the human STN corroborates the STN's participation in nonmotor circuits. The STN was previously shown to participate in different components of emotional processing, including emotion recognition and subjective feelings (4, 54). We confirm the importance of the STN as a hub within the limbic circuitry involved in both emotional valence and arousal processing as in two functionally and spatially segregated systems. This, together with our finding of several neurons involved separately in perceptual and emotional processing, support the complex role of the STN. Our results thus extend our knowledge of the STN's role in limbic circuits and contribute to a better understanding of the affective disturbances seen in PD patients treated with subthalamic stimulation.

## Experimental Procedures

**Subjects.** Thirteen PD patients (11 men, 2 women; mean age, 55.5 ± 8.7 y; age range, 42–69 y) undergoing bilateral electrode implantation for the STN DBS due to motor fluctuations and/or disabling dyskinesias were enrolled. The subjects had mean duration of PD of 14.2 ± 5.6 y (range, 9–30 y) and a mean motor score on the Unified Parkinson's Disease Rating Scale (UPDRS-III) in the off-medication condition of 38.7 ± 11.4 (range, 18–65) (Table 2). We also included another four patients undergoing bilateral electrode implantation for the globus pallidus interna DBS due to PD (Table S1), to study neuronal activity outside of the STN. All patients met the United Kingdom Brain Bank Criteria for diagnosis of PD. The study was approved by the Ethics Committee of the General University Hospital in Prague, Czech Republic, and all patients provided written informed consent for participation in the study.

Four days before surgery, dopamine agonists were substituted with equivalent doses of levodopa. All other anti-PD medications (e.g., amantadine, anticholinergics) had been suspended earlier during the preparation for surgery. Levodopa was withdrawn at least 12 h before the surgery. Five of the patients were receiving antidepressant therapy (1 on mianserin, 4 on citalopram), which was not discontinued. Patients with dementia and/or depression had been excluded by a routine psychiatric examination and neuropsychological testing (e.g., mini-mental state examination, Mattis dementia rating scale, Beck depression inventory).

**Affective Task.** Emotionally charged pictures of three categories were selected from the International Affective Picture System (IAPS) (80). The "pleasant" category included pictures with erotic themes (e.g., people, romantic couples) and adventure (e.g., exotic landscapes, animals, sports); the "unpleasant" category included pictures of victims (e.g., mutilations) and threats (e.g., human or animal attacks, aimed guns); and the "neutral" category comprised pictures of household objects, buildings, plants, and neutral faces, and scenes. Out of 144 unique pictures, six different variants of the task, each containing 24 pictures, were compiled involving 8 pictures from each category. Pleasant and unpleasant pictures were selected in a way such that they represented emotional stimuli scaled from weak to strong according to normative emotional valence and arousal. In addition, the pictures were organized pseudorandomly, so that no more than two pictures from one category followed in sequence. Each picture was presented for 2 s, preceded by a black screen with a white cross in the center for various durations (3,500–5,500 ms). Patients were instructed to fix their eyes on the cross on the black screen and to simply watch the pictures presented and remain motionless until the end of the task.

**Surgery and Intraoperative Microrecording.** DBS electrodes (model 3389; Medtronic) were implanted bilaterally under local anesthesia, guided by stereotactic magnetic resonance, microelectrode recordings (MERs), and macroelectrode intraoperative stimulation as described elsewhere (81, 82). Presurgical planning was done with the SurgiPlan software system (Elekta) and was based on coregistration of preoperative frameless 3.0-T MRI using T1-weighted images (MP-RAGE sequence; 160 sagittal slices, 1.0 mm thick, with x-y resolution 1 × 1 mm; TR, 2,300 ms; TE, 4.4 ms; FA, 10 degrees) and T2-weighted images (28 axial slices and 21 coronal slices, 2 mm thick, with x-y resolution 0.9 × 0.9 mm; TR, 2,430 ms; TE, 80 ms) with preoperative frame-based 1.5-T T1-weighted images (MP-RAGE sequence; 160 sagittal slices, 1.25 mm thick, with x-y resolution 1 × 1 mm; TR, 2,500 ms; TE, 3.1 ms; FA, 45 degrees) obtained immediately before the surgical procedure with the stereotactic Leksell frame attached.

The central trajectory of the exploratory microelectrode was aimed at the STN center near the anterior part of the red nucleus. Extracellular single-neuron activity was mapped by the MER using parallel insertion of five tungsten microelectrodes spaced 2 mm apart in a "Ben-gun" configuration to select sites for macroelectrode intraoperative stimulation. The five parallel microelectrodes were advanced simultaneously with a motor microdrive in 0.5-mm steps, beginning at 10 mm above the target. Depending on the length of STN-positive signals, the MERs were extended ∼2–3 mm beyond the STN. Four out of five channels of the Leadpoint recording system (Medtronic) were used for the MERs, filtered with a 500-Hz high-pass filter and a 5-kHz low-pass filter, sampled at 24 kHz, and stored for off-line processing. Single-channel electrooculography was performed for analysis of eye movement-related neuronal activity (83).

In up to six regions with an easily classifiable neuronal pattern specific for STN, the neuronal activity was recorded during the affective task presentation with a unique variant of affective pictures in each position. The number of positions depended on the time course of the surgery and on the patient's preference, clinical condition, and compliance. Patients were observed during the affective task, and if there appeared to be any distracting discomfort or sleepiness during surgery, then the experiment was abbreviated or not performed. The affective task was presented on a 17″ computer screen placed approximately 55 cm in front of the patient's eyes, with the patient laying motionless in the supine position, as is customary for this surgical procedure. The MER signals were acquired in 2-s epoch intervals recorded during both the picture presentation (PIC epoch) and the black screen presentation (FIX epoch), producing a sequence of 48 MER epochs ($FIX_1$, $PIC_1$, ..., $FIX_{24}$, $PIC_{24}$) for a total duration of 96 s.

**Rating of Emotional Valence and Arousal.** A subjective rating of the emotional content of the pictures was not elicited during the surgery, to avoid possible contamination of neuronal activity by voluntary movements during the rating process. Emotional valence and arousal ratings for each picture in the task were assessed before the initiation of chronic DBS at 4–5 wk after implantation, with a sufficient delay after surgery to allow cessation of any transitory microlesion effect related to penetration of the DBS electrode (84). No patient had any change in medication regimen after the surgery. Patients were assessed under similar conditions as during surgery in the off-stimulation and off-medication states (after withdrawal of dopaminergic treatment for at least 12 h).

Each picture was presented on a touch-sensitive screen for a 6-s period. The patients were instructed to look at each picture and to rate it along the dimensions of emotional valence and arousal by self-paced touching of appropriate symbols on two independent visual scales presented on-screen after picture offset. The scales were designed according to the original IAPS scales. Valence was rated on a scale of 1–9, with 9 representing the most pleasant stimulus, and arousal was also rated on a scale of 1–9, with 9 the most arousing stimulus.

**Data Analysis.** WaveClus (85), an unsupervised spike detection and sorting tool that has performed reasonably well on single-channel MERs (86), was used to extract the series of action potentials of single neurons from MER signals. Neurons related to eye movements were excluded from further analysis (83). For other neurons, the alpha band activity expressing the magnitude of 8–12 Hz periodic increases and decreases in the intensity of neuronal firing was computed as described below. The number of action potentials in 5-ms segments was calculated and concatenated to form a discrete signal representing the instantaneous intensity of firing. The signal was standardized to zero mean, and fast Fourier transform was carried out, applying a Hann window of length 100 with 75% overlap. The alpha band (8–12 Hz) spectral component of the signal was then extracted (Fig. S1), and alpha band activity was defined as the mean power of the alpha band spectral component, subjected to the square root transform to stabilize variance.

To detect neurons with emotion-related activity, we built linear models of the alpha band activity obtained during PIC epochs in the 500–2,000 ms interval after picture onset. To find valence-related neurons, we built a model of the alpha band activity during PIC epochs for each neuron using three covariates: (*i*) valence ratings, (*ii*) alpha band activity in the previous FIX epoch, and (*iii*) alpha band activity in the previous PIC epoch. The latter two covariates were included to adjust for past activity, given that a strong serial correlation was present in alpha band activity (*SI Experimental Procedures* and Fig. S5).

To find arousal-related neurons, we created another model of alpha band activity during PIC epochs for each neuron using five covariates: (*i*) arousal rating, (*ii*) alpha band activity in the previous FIX epoch, (*iii*) alpha band activity in the previous PIC epoch, and (*iv* and *v*) two categorical covariates adjusting for the picture category (positive vs. neutral, negative vs. neutral). We hypothesized that pictures of the same arousal but of distinct categories could provoke activities of different intensity. A neuron was considered to be related to valence (arousal) if the valence (arousal) covariate in the respective model was significant. Interhemispheric differences in the number of neurons were tested using the $\chi^2$ test of proportions.

To detect neurons sensitive to visual stimuli, we analyzed differences in the alpha band activity between the FIX epoch and the 0–500 ms interval of the following PIC epoch using the paired *t* test.

Each neuron was finally mapped into reference STN space by assessing the position of the neuron within the patient's STN and then aligning each STN with the model (30). To assess the position of a neuron within the STN, the preoperative STN-delineating frame-based MRI used for presurgical planning was coregistered with a frameless postoperative MRI displaying the position of the permanent electrode being in a known position relative to the microelectrode used for the MERs. To align each STN with the model, 12 points anatomically delineating the STN and the anterior and posterior commissures were identified in both the model and the preoperative T2-weighted MRI, and then fitted to one another by a linear transform (*SI Experimental Procedures* and Tables S2 and S3). A permutation test was used to assess the difference in the relative location of valence-related and arousal-related neurons.

Data processing and analyses were performed with MATLAB R2007b (MathWorks) and R statistical software (87).

**ACKNOWLEDGMENTS.** We thank Markéta Fialová, Anna Rezková, and Martin Voleman for administrative and technical support. This work was supported by the Czech Ministry of Education [Grant LH13256 (VES13-KontaktII)], the Czech Science Foundation (Grant Project 309/09/1145), the Czech Ministry of Health (Grant IGA MZ ČR NT12282-5/2011; Research Project MŠM 0021620849), the Charles University in Prague (Research Project PRVOUK-P26/LF1/4), and the European Social Fund (within the framework of realizing the project "Support of Inter-Sectoral Mobility and Quality Enhancement of Research Teams at Czech Technical University in Prague"; CZ.1.07/2.3.00/30.0034).

1. Okun MS (2012) Deep-brain stimulation for Parkinson's disease. *N Engl J Med* 367(16):1529–1538.
2. Alexander GE, Crutcher MD, DeLong MR (1990) Basal ganglia-thalamocortical circuits: Parallel substrates for motor, oculomotor, "prefrontal" and "limbic" functions. *Prog Brain Res* 85:119–146.
3. Voon V, Kubu C, Krack P, Houeto JL, Tröster AI (2006) Deep brain stimulation: Neuropsychological and neuropsychiatric issues. *Mov Disord* 21(Suppl 14):S305–S327.
4. Castrioto A, Lhommée E, Moro E, Krack P (2014) Mood and behavioural effects of subthalamic stimulation in Parkinson's disease. *Lancet Neurol* 13(3):287–305.
5. Dujardin K, et al. (2004) Subthalamic nucleus stimulation induces deficits in decoding emotional facial expressions in Parkinson's disease. *J Neurol Neurosurg Psychiatry* 75(2):202–208.
6. Schneider F, et al. (2003) Deep brain stimulation of the subthalamic nucleus enhances emotional processing in Parkinson disease. *Arch Gen Psychiatry* 60(3):296–302.
7. Kühn AA, et al. (2005) Activation of the subthalamic region during emotional processing in Parkinson disease. *Neurology* 65(5):707–713.
8. Schroeder U, et al. (2004) Facial expression recognition and subthalamic nucleus stimulation. *J Neurol Neurosurg Psychiatry* 75(4):648–650.
9. Baunez C, Amalric M, Robbins TW (2002) Enhanced food-related motivation after bilateral lesions of the subthalamic nucleus. *J Neurosci* 22(2):562–568.
10. Rouaud T, et al. (2010) Reducing the desire for cocaine with subthalamic nucleus deep brain stimulation. *Proc Natl Acad Sci USA* 107(3):1196–1200.
11. Serranová T, et al. (2011) Subthalamic nucleus stimulation affects incentive salience attribution in Parkinson's disease. *Mov Disord* 26(12):2260–2266.
12. Serranová T, et al. (2013) Sex, food and threat: Startling changes after subthalamic stimulation in Parkinson's disease. *Brain Stimul* 6(5):740–745.
13. Karama S, Armony J, Beauregard M (2011) Film excerpts shown to specifically elicit various affects lead to overlapping activation foci in a large set of symmetrical brain regions in males. *PLoS ONE* 6(7):e22343.
14. Frühholz S, Grandjean D (2012) Towards a fronto-temporal neural network for the decoding of angry vocal expressions. *Neuroimage* 62(3):1658–1666.
15. Kawasaki H, et al. (2005) Analysis of single-unit responses to emotional scenes in human ventromedial prefrontal cortex. *J Cogn Neurosci* 17(10):1509–1518.
16. Laxton AW, et al. (2013) Neuronal coding of implicit emotion categories in the subcallosal cortex in patients with depression. *Biol Psychiatry* 74(10):714–719.
17. Ojemann JG, Ojemann GA, Lettich E (1992) Neuronal activity related to faces and matching in human right nondominant temporal cortex. *Brain* 115(Pt 1):1–13.
18. Wang S, et al. (2014) Neurons in the human amygdala selective for perceived emotion. *Proc Natl Acad Sci USA* 111(30):E3110–E3119.
19. Russell JA (2003) Core affect and the psychological construction of emotion. *Psychol Rev* 110(1):145–172.
20. Lang PJ, Bradley MM, Cuthbert BN (1998) Emotion, motivation, and anxiety: Brain mechanisms and psychophysiology. *Biol Psychiatry* 44(12):1248–1263.

21. Lang PJ, Greenwald MK, Bradley MM, Hamm AO (1993) Looking at pictures: Affective, facial, visceral, and behavioral reactions. *Psychophysiology* 30(3):261–273.
22. Hamann S, Canli T (2004) Individual differences in emotion processing. *Curr Opin Neurobiol* 14(2):233–238.
23. Degos B, Deniau JM, Chavez M, Maurice N (2009) Chronic but not acute dopaminergic transmission interruption promotes a progressive increase in cortical beta frequency synchronization: Relationships to vigilance state and akinesia. *Cereb Cortex* 19(7): 1616–1630.
24. Bergman H, Wichmann T, Karmon B, DeLong MR (1994) The primate subthalamic nucleus, II: Neuronal activity in the MPTP model of parkinsonism. *J Neurophysiol* 72(2):507–520.
25. Jenkinson N, Brown P (2011) New insights into the relationship between dopamine, beta oscillations and motor function. *Trends Neurosci* 34(12):611–618.
26. Huebl J, et al. (2014) Oscillatory subthalamic nucleus activity is modulated by dopamine during emotional processing in Parkinson's disease. *Cortex* 60:69–81.
27. Brown P, Williams D (2005) Basal ganglia local field potential activity: Character and functional significance in the human. *Clin Neurophysiol* 116(11):2510–2519.
28. Brücke C, et al. (2007) The subthalamic region is activated during valence-related emotional processing in patients with Parkinson's disease. *Eur J Neurosci* 26(3):767–774.
29. Huebl J, et al. (2011) Modulation of subthalamic alpha activity to emotional stimuli correlates with depressive symptoms in Parkinson's disease. *Mov Disord* 26(3):477–483.
30. Morel A (2007) *Stereotactic Atlas of the Human Thalamus and Basal Ganglia* (Informa Healthcare, London), p 160.
31. Bradley MM, Codispoti M, Lang PJ (2006) A multi-process account of startle modulation during affective perception. *Psychophysiology* 43(5):486–497.
32. Adolphs R (2002) Neural systems for recognizing emotion. *Curr Opin Neurobiol* 12(2): 169–177.
33. Guillory SA, Bujarski KA (2014) Exploring emotions using invasive methods: Review of 60 years of human intracranial electrophysiology. *Soc Cogn Affect Neurosci* 9(12): 1880–1889.
34. Schupp HT, Junghöfer M, Weike AI, Hamm AO (2004) The selective processing of briefly presented affective pictures: An ERP analysis. *Psychophysiology* 41(3):441–449.
35. Junghöfer M, Bradley MM, Elbert TR, Lang PJ (2001) Fleeting images: A new look at early emotion discrimination. *Psychophysiology* 38(2):175–178.
36. D'Hondt F, et al. (2010) Early brain-body impact of emotional arousal. *Front Hum Neurosci* 4:33.
37. Burgmer M, et al. (2013) Early affective processing in patients with acute posttraumatic stress disorder: Magnetoencephalographic correlates. *PLoS ONE* 8(8):e71289.
38. Cacioppo JT, Petty RE, Losch ME, Kim HS (1986) Electromyographic activity over facial muscle regions can differentiate the valence and intensity of affective reactions. *J Pers Soc Psychol* 50(2):260–268.
39. Vrana SR, Spence EL, Lang PJ (1988) The startle probe response: A new measure of emotion? *J Abnorm Psychol* 97(4):487–491.
40. Kuhbandner C, Zehetleitner M (2011) Dissociable effects of valence and arousal in adaptive executive control. *PLoS ONE* 6(12):e29287.
41. Faure A, Reynolds SM, Richard JM, Berridge KC (2008) Mesolimbic dopamine in desire and dread: Enabling motivation to be generated by localized glutamate disruptions in nucleus accumbens. *J Neurosci* 28(28):7184–7192.
42. Anders S, Lotze M, Erb M, Grodd W, Birbaumer N (2004) Brain activity underlying emotional valence and arousal: A response-related fMRI study. *Hum Brain Mapp* 23(4):200–209.
43. Colibazzi T, et al. (2010) Neural systems subserving valence and arousal during the experience of induced emotions. *Emotion* 10(3):377–389.
44. Small DM, et al. (2003) Dissociation of neural representation of intensity and affective valuation in human gustation. *Neuron* 39(4):701–711.
45. Anderson AK, et al. (2003) Dissociated neural representations of intensity and valence in human olfaction. *Nat Neurosci* 6(2):196–202.
46. Bradley MM, Codispoti M, Cuthbert BN, Lang PJ (2001) Emotion and motivation I: Defensive and appetitive reactions in picture processing. *Emotion* 1(3):276–298.
47. Winston JS, Gottfried JA, Kilner JM, Dolan RJ (2005) Integrated neural representations of odor intensity and affective valence in human amygdala. *J Neurosci* 25(39): 8903–8907.
48. Roy M, Shohamy D, Wager TD (2012) Ventromedial prefrontal-subcortical systems and the generation of affective meaning. *Trends Cogn Sci* 16(3):147–156.
49. Berridge KC, Kringelbach ML (2013) Neuroscience of affect: Brain mechanisms of pleasure and displeasure. *Curr Opin Neurobiol* 23(3):294–303.
50. Grabenhorst F, Rolls ET (2011) Value, pleasure and choice in the ventral prefrontal cortex. *Trends Cogn Sci* 15(2):56–67.
51. Smith KS, Tindell AJ, Aldridge JW, Berridge KC (2009) Ventral pallidum roles in reward and motivation. *Behav Brain Res* 196(2):155–167.
52. Humphries MD, Prescott TJ (2010) The ventral basal ganglia, a selection mechanism at the crossroads of space, strategy, and reward. *Prog Neurobiol* 90(4):385–417.
53. Haber SN, Knutson B (2010) The reward circuit: Linking primate anatomy and human imaging. *Neuropsychopharmacology* 35(1):4–26.
54. Péron J, Frühholz S, Vérin M, Grandjean D (2013) Subthalamic nucleus: A key structure for emotional component synchronization in humans. *Neurosci Biobehav Rev* 37(3): 358–373.
55. Baunez C, Yelnik J, Mallet L (2011) Six questions on the subthalamic nucleus: Lessons from animal models and from stimulated patients. *Neuroscience* 198:193–204.
56. Haynes WI, Haber SN (2013) The organization of prefrontal-subthalamic inputs in primates provides an anatomical substrate for both functional specificity and integration: Implications for basal ganglia models and deep brain stimulation. *J Neurosci* 33(11):4804–4814.
57. Nambu A, Tokuno H, Takada M (2002) Functional significance of the cortico-subthalamo-pallidal "hyperdirect" pathway. *Neurosci Res* 43(2):111–117.
58. Parent A, Hazrati LN (1995) Functional anatomy of the basal ganglia, II: The place of subthalamic nucleus and external pallidum in basal ganglia circuitry. *Brain Res Brain Res Rev* 20(1):128–154.
59. Groenewegen HJ, Berendse HW (1990) Connections of the subthalamic nucleus with ventral striatopallidal parts of the basal ganglia in the rat. *J Comp Neurol* 294(4): 607–622.
60. Winter C, et al. (2008) High-frequency stimulation of the subthalamic nucleus modulates neurotransmission in limbic brain regions of the rat. *Exp Brain Res* 185(3): 497–507.
61. Turner MS, Lavin A, Grace AA, Napier TC (2001) Regulation of limbic information outflow by the subthalamic nucleus: Excitatory amino acid projections to the ventral pallidum. *J Neurosci* 21(8):2820–2832.
62. Ghashghaei HT, Hilgetag CC, Barbas H (2007) Sequence of information processing for emotions based on the anatomic dialogue between prefrontal cortex and amygdala. *Neuroimage* 34(3):905–923.
63. Lambert C, et al. (2012) Confirmation of functional zones within the human subthalamic nucleus: Patterns of connectivity and sub-parcellation using diffusion-weighted imaging. *Neuroimage* 60(1):83–94.
64. Wager TD, Phan KL, Liberzon I, Taylor SF (2003) Valence, gender, and lateralization of functional brain anatomy in emotion: A meta-analysis of findings from neuroimaging. *Neuroimage* 19(3):513–531.
65. Lindquist KA, Wager TD, Kober H, Bliss-Moreau E, Barrett LF (2012) The brain basis of emotion: A meta-analytic review. *Behav Brain Sci* 35(3):121–143.
66. Frühholz S, Grandjean D (2013) Multiple subregions in superior temporal cortex are differentially sensitive to vocal expressions: A quantitative meta-analysis. *Neurosci Biobehav Rev* 37(1):24–35.
67. Eitan R, et al. (2013) Asymmetric right/left encoding of emotions in the human subthalamic nucleus. *Front Syst Neurosci* 7:69.
68. Karachi C, et al. (2005) The pallidosubthalamic projection: An anatomical substrate for nonmotor functions of the subthalamic nucleus in primates. *Mov Disord* 20(2): 172–180.
69. Joel D, Weiner I (1997) The connections of the primate subthalamic nucleus: Indirect pathways and the open-interconnected scheme of basal ganglia-thalamocortical circuitry. *Brain Res Brain Res Rev* 23(1-2):62–78.
70. Brunenberg EJ, et al. (2012) Structural and resting state functional connectivity of the subthalamic nucleus: Identification of motor STN parts and the hyperdirect pathway. *PLoS ONE* 7(6):e39061.
71. Espinosa-Parrilla JF, Baunez C, Apicella P (2013) Linking reward processing to behavioral output: Motor and motivational integration in the primate subthalamic nucleus. *Front Comput Neurosci* 7:175.
72. Matsumura M, Kojima J, Gardiner TW, Hikosaka O (1992) Visual and oculomotor functions of monkey subthalamic nucleus. *J Neurophysiol* 67(6):1615–1632.
73. Coizet V, et al. (2009) Short-latency visual input to the subthalamic nucleus is provided by the midbrain superior colliculus. *J Neurosci* 29(17):5701–5709.
74. Rolland M, Carcenac C, Overton PG, Savasta M, Coizet V (2013) Enhanced visual responses in the superior colliculus and subthalamic nucleus in an animal model of Parkinson's disease. *Neuroscience* 252:277–288.
75. Jech R, et al. (2006) Deep brain stimulation of the subthalamic nucleus affects resting EEG and visual evoked potentials in Parkinson's disease. *Clin Neurophysiol* 117(5): 1017–1028.
76. Shires J, Joshi S, Basso MA (2010) Shedding new light on the role of the basal ganglia-superior colliculus pathway in eye movements. *Curr Opin Neurobiol* 20(6):717–725.
77. Tamietto M, de Gelder B (2010) Neural bases of the non-conscious perception of emotional signals. *Nat Rev Neurosci* 11(10):697–709.
78. Braak H, et al. (2002) Staging of the intracerebral inclusion body pathology associated with idiopathic Parkinson's disease (preclinical and clinical stages). *J Neurol* 249(Suppl 3):):III/1–III/5.
79. Péron J, Dondaine T, Le Jeune F, Grandjean D, Vérin M (2012) Emotional processing in Parkinson's disease: A systematic review. *Mov Disord* 27(2):186–199.
80. Lang PJ, Bradley MM, Cuthbert BN (2008) *International Affective Picture System (IAPS): Affective Ratings of Pictures and Instruction Manual* (University of Florida, Gainesville, FL), Technical Report A-8.
81. Gross RE, Krack P, Rodriguez-Oroz MC, Rezai AR, Benabid AL (2006) Electrophysiological mapping for the implantation of deep brain stimulators for Parkinson's disease and tremor. *Mov Disord* 21(Suppl 14):S259–S283.
82. Pollak P, et al. (2002) Intraoperative micro- and macrostimulation of the subthalamic nucleus in Parkinson's disease. *Mov Disord* 17(Suppl 3):S155–S161.
83. Sieger T, et al. (2013) Basal ganglia neuronal activity during scanning eye movements in Parkinson's disease. *PLoS ONE* 8(11):e78581.
84. Jech R, et al. (2012) The subthalamic microlesion story in Parkinson's disease: Electrode insertion-related motor improvement with relative cortico-subcortical hypoactivation in fMRI. *PLoS ONE* 7(11):e49056.
85. Quiroga RQ, Nadasdy Z, Ben-Shaul Y (2004) Unsupervised spike detection and sorting with wavelets and superparamagnetic clustering. *Neural Comput* 16(8):1661–1687.
86. Wild J, Prekopcsak Z, Sieger T, Novak D, Jech R (2012) Performance comparison of extracellular spike sorting algorithms for single-channel recordings. *J Neurosci Methods* 203(2): 369–376.
87. R Core Team (2013) *R: A Language and Environment for Statistical Computing* (R Foundation for Statistical Computing, Vienna).

# Supporting Information

## Sieger et al. 10.1073/pnas.1410709112

### SI Experimental Procedures

**Mapping of STN Neurons.** To map subthalamic neurons in the reference STN space, the position of each neuron in patients' individual STN was assessed, followed by fitting each STN onto the STN model (1). To determine the position of neurons in the patient's STN, first both the frameless preoperative 3.0-T T2-weighted MRI visualizing the STN (*Experimental Procedures*) and the frameless postoperative 1.5-T T1-weighted MRI displaying the susceptibility artifact of the permanent DBS electrode were automatically coregistered with the frame-based preoperative 1.5-T T1-weighted MRI used for neurosurgical planning (*Experimental Procedures*) in each patient using SurgiPlan software (Elekta), thereby placing all preoperative and postoperative images into one stereotactic space. The accuracy of the merge was always confirmed using the SurgiPlan "movable lens," enabling the user to visually examine two overlapping images by sweeping across the screen to convert from one to the other. The frameless postoperative 1.5-T T1-weighted MRI was acquired at ∼2–5 d after DBS implantation (MP-RAGE sequence, 160 axial slices, 1.65-mm thick, with x-y resolution 0.9 × 0.9 mm; TR, 2,140 ms; TE, 3.93 ms; and FA, 15 degrees).

Second, the position of the five parallel trajectories of microelectrodes used for perioperative microrecording was reconstructed based on the location of the T1-weighted MRI susceptibility artifact of the permanent DBS electrode and the known relative position of the trajectories with respect to the stimulation electrode from perioperative documentation. Finally, the position of each recorded neuron along each reconstructed trajectory was manually determined in the SurgiPlan software based on the known depth at which the neuron was identified.

To align each STN with the model, 12 points anatomically delineating the STN and 2 additional points, the anterior commissure (AC) and posterior commissure (PC), were identified in both the reference model (1) and the preoperative 3-T T2-weighted MRI, and then coregistered with the 14 corresponding points of the model using a linear mapping approach (see below). The reference model consisted of coronal slices of the STN manually digitized from the atlas (1) (Fig. S4*A*). Each individual STN was delineated manually in preoperative axial and coronal projections; the delineating points are defined in Table S2 and depicted in Fig. S4. The anteroposterior direction in both the model and the MRI was defined by the line connecting the AC and PC. All planes of view were used for accurate delineation of STN borders in Surgiplan.

The linear mapping involved aligning the centroid of the 12 corresponding points of each individual STN (together with AC and PC) with the analogous centroid in the STN model, followed by scaling in the mediolateral ($S_{ML}$), anteroposterior ($S_{AP}$), and ventrodorsal ($S_{VD}$) directions, and rotating around those three directions ($\alpha_{ML}$, $\alpha_{AP}$, and $\alpha_{VD}$). The scaling and rotation parameters were found by numerical optimization, minimizing the sum of square distances between the pairs of the delineating points in the patient's STN and the model starting from $S_{ML} = S_{AP} = S_{VD} = 100\%$ and $\alpha_{ML} = \alpha_{AP} = \alpha_{VD} = 0°$. A summary of the optimized parameters, given in Table S3, shows a reasonable match. On average, a patient's STN had to be scaled by <10% and rotated by <6° around each axis.

The accuracy of the mapping procedure was validated by comparing the borders of each STN, as identified in microelectrode recordings, with MRI-based STN reconstruction using the fitted model. The mean distance between points at which microelectrodes entered (and exited) the STN and the corresponding points interpolated on the STN model was 0.69 mm (IQR, 0.70 mm) and ranged from 0.01 to 2.54 mm, showing good accuracy of the mapping that is comparable to the results of other authors (2–4).

Several reasons might account for the observed mismatches between the microrecording-defined and MRI-defined STN borders in our study. First, the position of the microelectrode was inferred indirectly from the position of the DBS macroelectrode in postoperative MRI. Thus, it is not possible to rule out, among other factors, minor brain shifts in some patients during removal of the microelectrode and DBS macroelectrode insertion. Second, the delineation of the STN, which is hypointense in the T2-weighted MRI owing to the presence of iron, is not always clear on the scans, because there are other iron-containing structures running close to the STN (4). Moreover, the distribution of iron deposition is uneven in the nucleus, and thus T2 hypointensity does not utterly correspond to the nuclei (5), and the T2-weighted MRI can be locally distorted by the presence of iron (6).

**Serial Correlation in Alpha Band Activity.** For each neuron, linear models were built explaining the present activity in the interval of 500–2,000 ms after the emotional picture onset (=PIC epoch) by particular type of past activity, and the significance of the explanatory past activity and the $R^2$ coefficient of determination expressing the percentage of the present activity explained by the past activity were computed for each model. The observed $R^2$ coefficients were compared with those expected assuming the present activity to be independent of past activity.

Serial correlation in alpha band activity was found, as illustrated by the increased $R^2$ coefficients of determination in models predicting the present activity in terms of past activity (Fig. S5). Among 90 STN neurons, the past activity in the interval of 0–2,000 ms during the blank screen presentation with a fixation cross (=$FIX_i$ epoch), $PIC_{i-1}$, $FIX_{i-1}$, and $PIC_{i-2}$ epochs predicted the activity in $PIC_i$ epochs in a significant number of 12, 10, 12, and 10 neurons, respectively ($P < 0.05$, binomial test). Serial correlation was detected over periods of up to 13 s.


1. Morel A (2007) *Atlas of the Human Thalamus and Basal Ganglia* (Informa Healthcare, London), p 160.
2. Bardinet E, et al. (2009) A three-dimensional histological atlas of the human basal ganglia, II: Atlas deformation strategy and evaluation in deep brain stimulation for Parkinson disease. *J Neurosurg* 110(2):208–219.
3. Hamani C, et al. (2005) Correspondence of microelectrode mapping with magnetic resonance imaging for subthalamic nucleus procedures. *Surg Neurol* 63(3):249–253, discussion 253.
4. Schlaier JR, et al. (2013) The influence of intraoperative microelectrode recordings and clinical testing on the location of final stimulation sites in deep brain stimulation for Parkinson's disease. *Acta Neurochir (Wien)* 155(2):357–366.
5. Dormont D, et al. (2004) Is the subthalamic nucleus hypointense on T2-weighted images? A correlation study using MR imaging and stereotactic atlas data. *AJNR Am J Neuroradiol* 25(9):1516–1523.
6. Menuel C, et al. (2005) Characterization and correction of distortions in stereotactic magnetic resonance imaging for bilateral subthalamic stimulation in Parkinson disease. *J Neurosurg* 103(2):256–266.

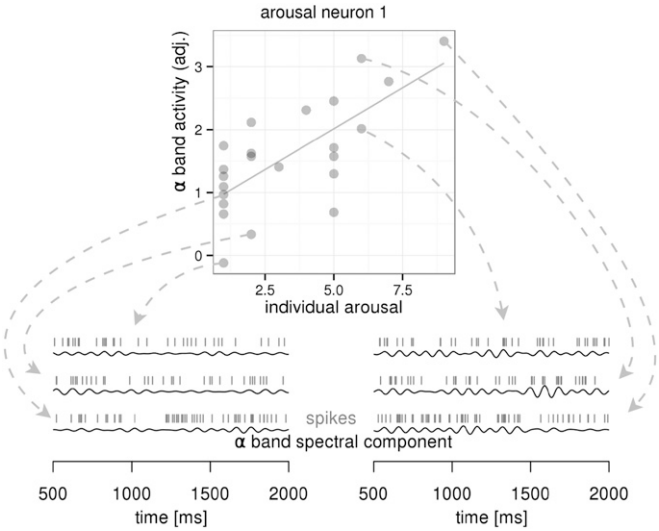


**Fig. S1.** Examples of neuronal firing and the alpha band spectral component of the instantaneous intensity of firing in six selected epochs recorded in the arousal-related neuron 1 (Fig. 2). The spikes are shown as vertical bars, the derived alpha band component of the firing intensity is plotted as a continuous curve beneath the spikes. Note that the amplitude and power of the alpha band spectral components (and thus the alpha band neuronal activity derived from it (*Experimental Procedures*) are much lower for the traces on the left side than for the traces on the right side.

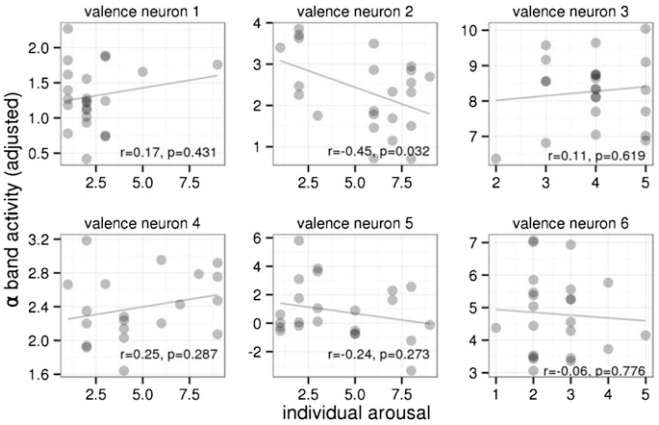


**Fig. S2.** Relationship of the single-neuron alpha band activity during emotional picture presentation (in the interval of 500–2,000 ms after picture onset) to the individual arousal ratings of the presented pictures in the six valence-related neurons of the STN (Fig. 1). The horizontal axis shows the individual ratings of the pictures' arousal, varying from 1 (low) to 9 (high). The vertical axis shows the alpha band neuronal activity adjusted for past activity and picture category (*Experimental Procedures*). For visualization purposes, correlation coefficients and their significance are included. Despite the fact that the correlation was significant in one neuron, none of these neurons was determined to be related to the individual arousal ratings using linear models.

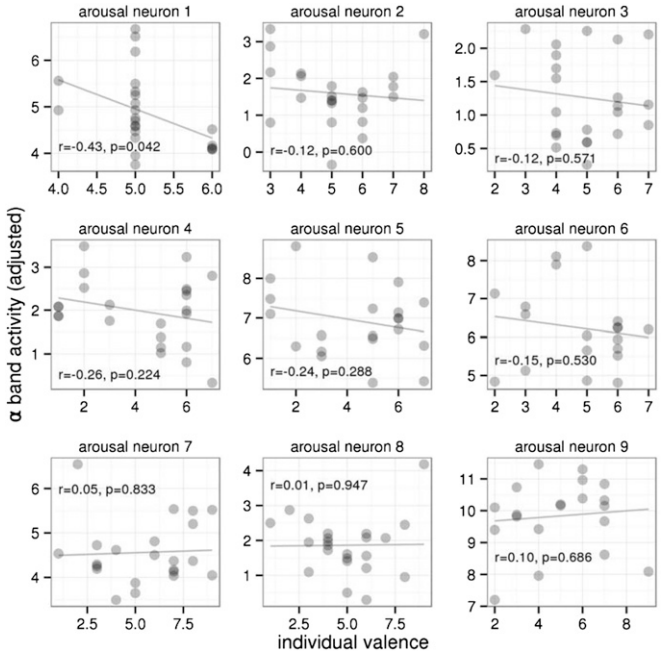


**Fig. S3.** Relationship of the single-neuron alpha band activity during emotional picture presentation (in the interval of 500–2,000 ms after picture onset) to the individual valence ratings of the presented pictures in the nine arousal-related neurons of the STN (Fig. 2). The horizontal axis shows the individual ratings of the pictures' valence, varying from 1 (unpleasant) to 9 (pleasant). The vertical axis shows the alpha band neuronal activity adjusted for past activity (*Experimental Procedures*). For visualization purposes, correlation coefficients and their significance are included. Despite the fact that the correlation was significant in one neuron, none of these neurons was determined to be related to the individual valence ratings using linear models.

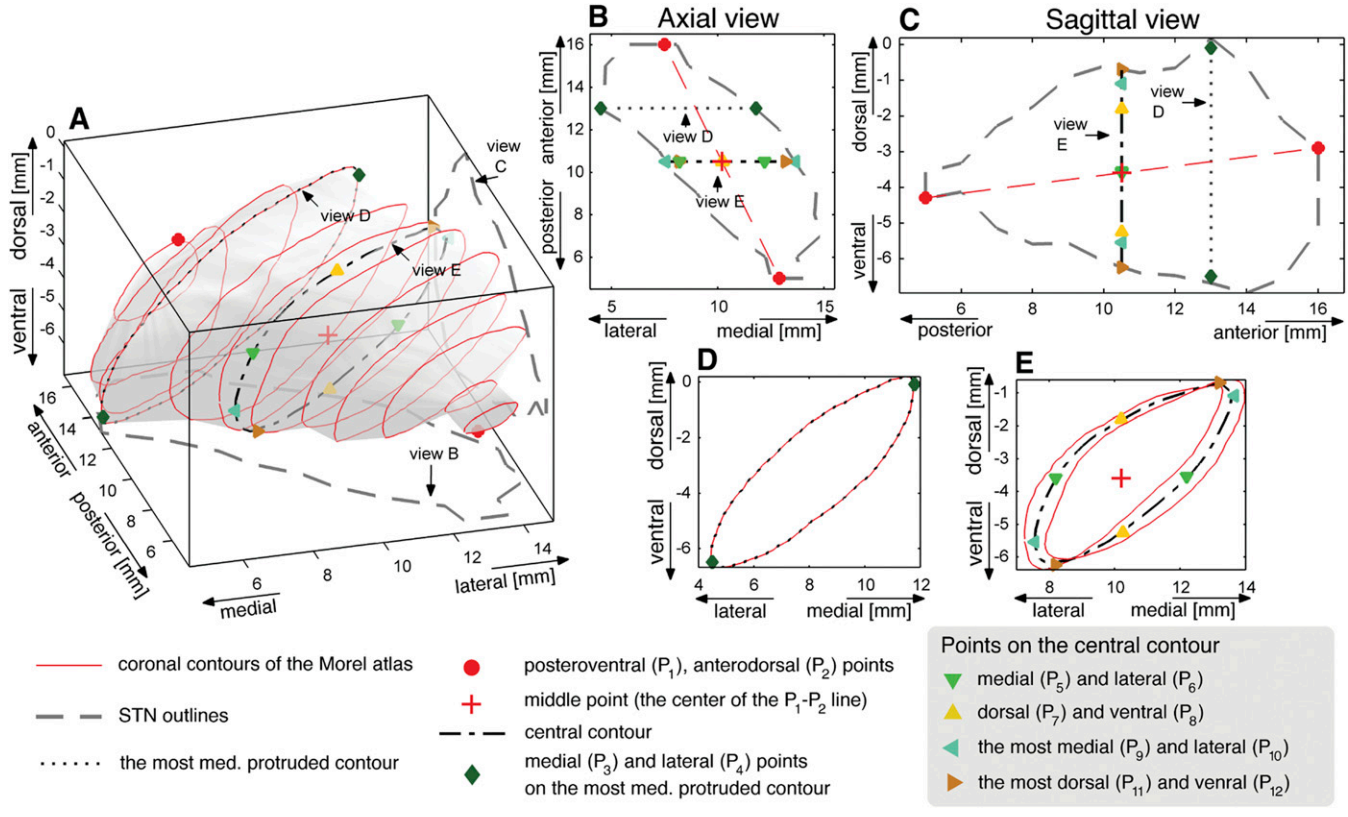


**Fig. S4.** Delineating points of the STN used to map each patient's STN onto the reference STN model (1). (*A*) Three-dimensional overview of the delineating points overlaid on the coronal contours of the model. (*B*) Axial view of the middle portion of the STN. (*C*) Sagittal view of the middle portion of the STN. (*D*) The most medially protruded slice in the anterior part of the STN. (*E*) The middle coronal slice of the STN model, defined by interpolating the two nearest model contours. Table S2 presents the exact definitions of the delineating points.

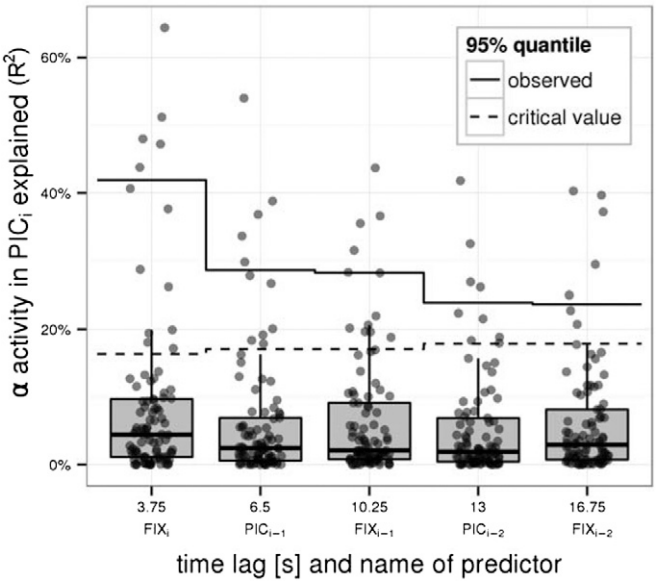


**Fig. S5.** Serial correlation in alpha band activity as expressed by the ability of past activity to predict present activity. The percentage of activity during the interval of 500–2,000 ms after picture onset (=PIC$_i$ epochs) on the vertical axis explained by particular types of past activity on the horizontal axis is shown for each of 90 STN neurons. The observed percentages are summarized by boxplots and 95% quantiles (solid line) and contrasted with their critical value (dashed line), computed assuming the present activity to be independent of the past activity. Covariates predicting the activity in PIC$_i$ epochs included, from left to right, the 0–2,000 ms interval of blank screen presentation with the fixating cross (=FIX$_i$ epochs) immediately preceding the PIC$_i$ epochs, the previous PIC$_{i-1}$ epochs, the FIX$_{i-1}$ epochs preceding the previous PIC$_{i-1}$ epochs, and so on. Serial correlation was present over periods of up to 13 s.

**Table S1. Description of patients with PD in whom globus pallidus neuronal activity was explored**

| Patient | Age, y | DD, y | Levodopa, mg | UPDRS-III | H-Y | GP neurons, n |
|---|---|---|---|---|---|---|
| 1 | 63 | 12 | 2,100 | 29 | 2 | 3 |
| 2 | 53 | 9 | 2,180 | 30 | 3 | 7 |
| 3 | 28 | 3 | 920 | 13 | 2 | 2 |
| 4 | 44 | 10 | 1,325 | 23 | 2 | 2 |

Age refers to age on the day of surgery; DD, PD duration; levodopa, dose/day in mg, including the levodopa-equivalent dosage of dopamine agonist (patient 1 was also treated with citalopram, and patient 4 was also treated with bupropion); UPDRS-III, motor score of the Unified Parkinson's Disease Rating Scale in the off-medication condition; H-Y, Hoehn and Yahr stage in the off-medication condition; GP neurons, neurons in the globus pallidus unrelated to eye movements.

**Table S2. Definition of the points anatomically delineating the STN**

| STN delineating point | Position |
|---|---|
| $P_1$ | Most ventral point in the posterior boundary |
| $P_2$ | Most dorsal point in the anterior boundary |
| $P_3$ | Most medial point in the in the most medially protruded slice in the anterior part of the STN |
| $P_4$ | Most lateral point in the most medially protruded slice in the anterior part of the STN |
| $P_5$ | Medial intersection of the axial plane crossing the middle point* and the middle contour† |
| $P_6$ | Lateral intersection of the of the axial plane crossing the middle point* and the middle contour† |
| $P_7$ | Dorsal intersection of the sagittal plane crossing the middle point* and the middle contour† |
| $P_8$ | Ventral intersection of the sagittal plane crossing the middle point* and the middle contour† |
| $P_9$ | Most medial point on the middle contour† |
| $P_{10}$ | Most lateral point on the middle contour† |
| $P_{11}$ | Most dorsal point on the middle contour† |
| $P_{12}$ | Most ventral point on the middle contour† |

These points were used to map the patients' STN onto the reference Morel STN atlas.
*The middle point is the center of the line connecting points $P_1$ and $P_2$.
†The middle contour is the coronal contour intersecting the middle point. In the Morel atlas, in which there was no contour intersecting the middle point, the middle contour was based on the interpolation of the two nearest contours.

**Table S3. Summary of the parameters of the linear mapping between each individual STN and the reference STN model (1) in PD**

| Linear mapping parameter | Mean (SD) | Range (min; max) |
|---|---|---|
| $S_{ML}$, % | 91 (8) | 75; 109 |
| $S_{AP}$, % | 98 (5) | 88; 106 |
| $S_{AP}$, % | 98 (8) | 85; 117 |
| $\alpha_{ML}$, ° | −1.3 (3.0) | −7.5; 5.4 |
| $\alpha_{AP}$, ° | 5.2 (5.1) | −2.3; 18.3 |
| $\alpha_{VD}$, ° | 1.4 (5.3) | −7.7; 8.7 |

Mean (SD) and minimum and maximum values for scaling in the mediolateral ($s_{ML}$), anteroposterior ($s_{AP}$), and ventrodorsal ($s_{VD}$) directions and rotation along these three directions ($\alpha_{ML}$, $\alpha_{AP}$, and $\alpha_{VD}$).